

## Magnetic Resonance Determination of the Antiferromagnetic Coupling of Fe Layers through Cr

J. J. Krebs, P. Lubitz, A. Chaiken, and G. A. Prinz

Naval Research Laboratory, Washington, D.C. 20375

(Received 5 July 1989)

Variable frequency ferromagnetic resonance (FMR) has been used to directly observe the coupled resonance modes in single-crystal Fe/Cr/Fe(001) sandwiches grown by molecular-beam epitaxy. Magnetization  $M$  and magnetoresistance measurements also were carried out on these samples, which exhibited antiferromagnetic (AF) layer alignment for  $12 < t(\text{Cr}) < 25 \text{ \AA}$ . The FMR data reveal two resonance modes with complex frequency dependences for the AF-aligned samples. The detailed FMR and  $M$  vs  $H$  behavior can be quantitatively explained by an AF coupling parameter  $J$  which has a thickness dependence peaked about  $t(\text{Cr}) = 16 \text{ \AA}$ .

PACS numbers: 75.70.-i, 72.15.Gd, 75.60.Ej, 76.50.+g

Very thin multiple films of Fe with intervening Cr films less than  $20 \text{ \AA}$  thick have recently generated considerable interest since they exhibit a clearcut antiferromagnetic alignment of the total moments of adjacent Fe layers.<sup>1-4</sup> They also exhibit unusual magnetoresistance effects which depend on the relative orientation of the magnetization in such layers.<sup>4-6</sup> Although neither the mechanism for the magnetoresistance, nor the basis of the coupling is as yet clearly understood, the antiferromagnetic coupling constant  $J$  and the magnetoresistance are both significantly enhanced when the Fe/Cr bilayer is repeated many times.<sup>4-6</sup> There is some conflict, however, in the reported dependence on Cr thickness  $t(\text{Cr})$ .

With these results in mind, we have prepared a large set of carefully grown single-crystal samples of the simple model bcc system Fe(001)/Cr(001)/Fe(001) with different  $t(\text{Cr})$ . Detailed magnetization  $M$ , magnetoresistance (MR), and ferromagnetic resonance (FMR) measurements reveal a very rich static and dynamic behavior for the subset of samples which show antiferromagnetic alignment. For the first time, we show that a simple phenomenological model is able to account quantitatively for all the data by including a finite coupling  $J$ . The form of the coupling term and the unusual dependence of  $J$  on  $t(\text{Cr})$  set important limits on any future first-principles theory.

To reduce the likelihood of conflicting interpretations, we chose to grow simple Fe/Cr/Fe bilayers with symmetric boundaries by molecular-beam epitaxy. Starting with a well-polished GaAs(001) substrate, a ZnSe(001) epilayer about  $2000 \text{ \AA}$  thick was grown to achieve a very flat surface.<sup>7</sup> Subsequent single-crystal Fe, Cr, and Fe films were grown using a substrate temperature near  $20^\circ\text{C}$  and growth conditions similar to those of Baibich *et al.*<sup>5</sup> Finally, a polycrystalline ZnSe layer about  $1000 \text{ \AA}$  thick was deposited on the stack for symmetry and for protection against the atmosphere.

Reflection high-energy electron diffraction and Auger spectroscopy were used to establish single crystallinity in

all the metal layers and indicated detectable impurity signals only from N (on Cr) and O (on Fe), both of a few percent or less. The thickness of the various layers were controlled by monitoring the corresponding fluxes with a quadrupole mass analyzer and were measured after growth by means of x-ray fluorescence. For the samples discussed,  $t(\text{Fe1}) = t(\text{Fe2}) \cong 40 \text{ \AA}$ , while  $t(\text{Cr})$  lay in the range of  $4\text{--}85 \text{ \AA}$  for different samples. We found it difficult to determine  $t(\text{Cr})$  absolutely to better than  $\pm 1 \text{ \AA}$ .

The  $M$  versus magnetic field  $H$  magnetization loops of the  $1\text{-cm}^2$  samples were measured with a vibrating-sample magnetometer, while the ac magnetoresistance data were then taken with use of cleaved bars with [110] along the bar axis. Electrical four-point contacts were made via sputtered Au pads on the top ZnSe layer. The MR data will be presented in the form  $\Delta\rho/\rho \{ = [\rho(H) - \rho(0)]/\rho(0) \}$  vs  $H$ . Note that the current  $I$  is always along [110]. The zero-field resistivity is typically  $50 \mu\text{mcm}$ , comparable to previously reported values for Fe/Cr/Fe multilayers.<sup>5</sup>

Two kinds of FMR apparatus were used to obtain different types of information. A commercial 35-GHz spectrometer was used for angularly dependent FMR to determine the values of the anisotropy constants and the effective magnetization  $4\pi M'$  (which includes any perpendicular anisotropy) at large magnetic fields for which the moments of the two Fe layer are fully aligned and parallel. In order to determine the effect of  $J$  on the dynamic behavior of the samples, we also carried out FMR measurements using a variable frequency spectrometer in which the sample forms a shorting plate at the end of a coaxial line. Data were taken for frequencies in the range from 2 to 14 GHz. For each trace, the frequency was set at a fixed value and the ac field-modulated signal was detected with a lock-in amplifier as  $H$  was swept.

All the data presented in this paper were taken at room temperature and with  $H$  in the sample plane.

For ease of comparison, the  $M$  vs  $H$  data, the MR

Work of the U. S. Government

Not subject to U. S. copyright

data, and the variable frequency vs  $H$  FMR data are all presented on the same horizontal scale in Fig. 1 for a sample with  $t(\text{Cr})=13 \text{ \AA}$  and with  $\mathbf{H} \parallel [110]$  or  $[1\bar{1}0]$ . The magnetization results [Fig. 1(a)], which are initially linear in  $H$ , show a sudden jump at  $H=150 \text{ Oe}$  followed by a slow approach to saturation which occurs above the saturation break at  $H_b=1.13 \text{ kOe}$  marked by the vertical dashed line. The relative orientations of  $\mathbf{M}$  in the two Fe layers (assuming antiferromagnetic coupling) can be deduced easily and are shown schematically by the ar-

rows in the insets in Fig. 1(a). Note that the zero-field magnetization orientations are along the easy  $\langle 100 \rangle$  axes of the two Fe films.

The MR data are shown for both the  $\mathbf{H} \parallel [110] \parallel \mathbf{I}$  (longitudinal MR) and  $\mathbf{H} \parallel [1\bar{1}0] \perp \mathbf{I}$  (transverse MR) orientations in Fig. 1(b). Both curves show the same jump and slow approach to saturation as do the magnetization data but after the jump the two curves change in opposite senses with increasing  $H$ , consistent with the known behavior of the parallel and perpendicular anomalous magnetoresistance of Fe.<sup>8</sup>

In Fig. 1(c), the data points indicate the magnetic fields at which resonance was detected for each of the microwave frequencies studied. Note the complex shapes of the mode curves, the fact that they show anomalies at the same special magnetic fields found in Figs. 1(a) and 1(b), and that at some frequencies as many as six resonance lines can be observed as the field is swept. At any given magnetic field, however, only two resonance modes are observed.

All samples which show antiferromagnetic alignment show FMR,  $M$  vs  $H$ , and MR behavior similar to that described above. The magnetic field locations of the steps, their magnitudes, and the FMR signals vary with  $t(\text{Cr})$  through their dependence on the magnitude of  $J$  as indicated below. The FMR linewidths found for all the samples studied were independent of whether their Fe layers showed antiferromagnetic alignment or not and were typically as narrow or narrower than those we found for single Fe films of comparable thickness grown on ZnSe(001). Complete data were also taken for  $\mathbf{H} \parallel [100]$  but are not presented here for lack of space.

The behavior described above results from a competition between the effects of the external magnetic field which favors  $\mathbf{M} \parallel \mathbf{H}$ , the magnetocrystalline and shape anisotropy which favor  $\mathbf{M}$  along an in-plane  $\langle 100 \rangle$  axis, and the coupling which favors the magnetization of the two films  $\mathbf{M}_1$  and  $\mathbf{M}_2$  antiparallel. The energy density  $E$  of the sample can be written as

$$E = \frac{1}{2} (E_1 + E_2) + J \hat{\mathbf{M}}_1 \cdot \hat{\mathbf{M}}_2, \tag{1}$$

where

$$E_i = K_1 (\alpha_{1i}^2 \alpha_{2i}^2 + \alpha_{2i}^2 \alpha_{3i}^2 + \alpha_{3i}^2 \alpha_{1i}^2) + K_u \cos^2(\phi_i - \pi/4) + 2\pi M_{ni}^2 - \mathbf{M}_i \cdot \mathbf{H} \tag{2}$$

with  $\hat{\mathbf{M}}_i$  a unit vector along  $\mathbf{M}_i$  and  $M_{ni}$  is its component normal to the film,  $\alpha_{ji}$  the direction cosines of  $\mathbf{M}_i$ ,  $K_1$  the usual cubic anisotropy,  $K_u$  an in-plane anisotropy which is commonly found in very thin Fe films on GaAs or ZnSe,<sup>8</sup> and  $\phi_i$  the azimuthal angle between  $\mathbf{M}_i$  and  $[100]$ .

The total moment along  $\mathbf{H}$  (the vibrating-sample magnetometer signal) can be calculated by simultaneously minimizing Eq. (1) with respect to  $\phi_1$  and  $\phi_2$ . This analysis gives the following expression for the saturation

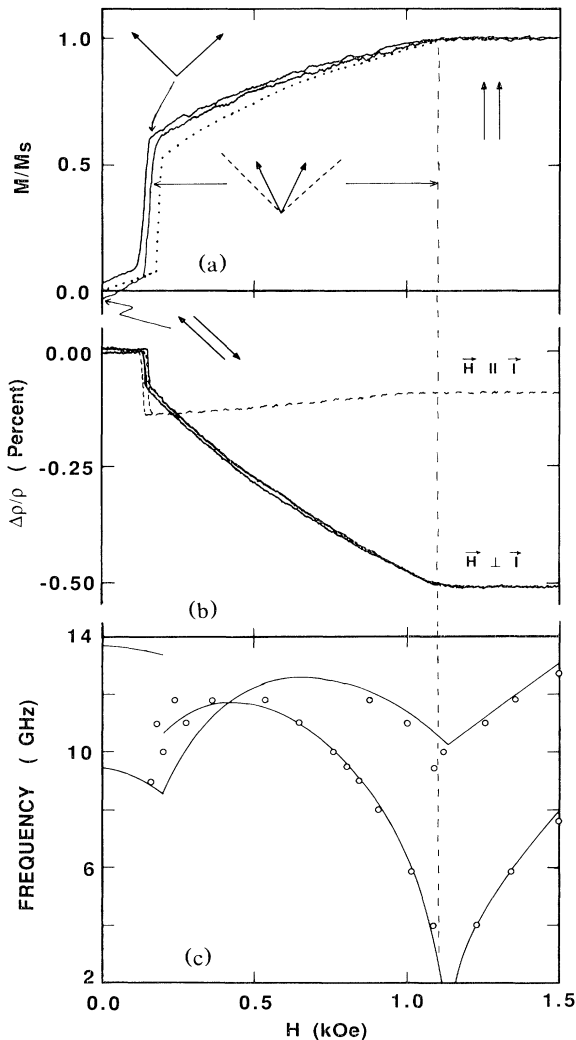


FIG. 1. Magnetic properties of a Fe/Cr/Fe(001) thin-film sample with  $t(\text{Cr})=13 \text{ \AA}$ . (a) Magnetization field dependence for  $\mathbf{H} \parallel [110]$ . Insets: Relative orientations of layer moments at points indicated. The vertical dashed line marks the saturation break  $H_b$ . The dotted line is a theoretical fit. (b) Longitudinal and transverse magnetoresistance. (c) Magnetic resonance data for  $\mathbf{H} \parallel [110]$ . Open circles are experimental; solid lines are from a theoretical calculation using the same parameter as in (a).

break at  $H_b$  (Fig. 1),

$$H_b = 4\tilde{J} + 2\tilde{K}_1 \pm 2\tilde{K}_u, \quad (3)$$

where  $\tilde{X} = X/M$ . Diény, Gavigan, and Rebouillat<sup>9</sup> have independently carried out a general analysis of the static  $M$  vs  $H$  behavior of a pair of antiferromagnetically coupled magnetic films and mapped out the stable  $\mathbf{M}_1, \mathbf{M}_2$  orientations in both  $(K_1/J, H/J)$  and  $(K_u/J, H/J)$  spaces. Where the two calculations overlap, our results agree well with theirs.

Using of the  $K_1, K_u$ , and  $4\pi M'$  values determined from the 35-GHz FMR measurements, together with  $J/M = 150$  Oe and taking  $\mathbf{H}$  along  $[110]$ , one calculates the theoretical  $M/M_s$  values indicated by the dotted line in Fig. 1(a). This one-parameter fit is quite good both as to the location and magnitude of the  $M$  vs  $H$  jump and the field dependence of  $M$ . If one were to set  $J=0$ , the  $M$  vs  $H$  signal would be expected *not* to have a jump and would saturate at  $H \cong 2K_1/M = 0.52$  kOe.

The dynamic FMR behavior of a pair of coupled ferromagnetic films also can be calculated using a method developed by Smit and Beljers<sup>10</sup> if an expression for the energy density  $E$  is known. For the saturated case with  $\mathbf{H} \parallel [1\bar{1}0]$  (or  $[110]$ ), one can show that the normal modes are the in-phase and out-of-phase precessions ( $\omega^+$  and  $\omega^-$ ) of  $\mathbf{M}_1$  and  $\mathbf{M}_2$ . In this special case, one can obtain explicit expressions for the corresponding frequencies, namely,<sup>11</sup>

$$(\omega^+/\gamma)^2 = [H + \tilde{K}_1 \pm 2\tilde{K}_u + 4\pi M'] \times [H - 2\tilde{K}_1 \pm 2\tilde{K}_u], \quad (4)$$

$$(\omega^-/\gamma)^2 = [H - 4\tilde{J} + \tilde{K}_1 \pm 2\tilde{K}_u + 4\pi M'] \times [H - 4\tilde{J} - 2\tilde{K}_1 \pm 2\tilde{K}_u], \quad (5)$$

where  $\gamma$  is the gyromagnetic ratio.

Using the same 35-GHz FMR values ( $K_1/M = 260$

TABLE I. The antiferromagnetic coupling parameter  $J/M$  as determined from  $M$  vs  $H$ , magnetoresistance, and high-field FMR data. Samples with  $t(\text{Cr}) = 4, 5, 7, 8, 10, \text{ or } 12 \text{ \AA}$  as well as those with  $t(\text{Cr}) = 25, 28, 36, 40 \text{ \AA}$  or thicker show no antiferromagnetic alignment. This implies that  $J/M \leq +0.02$  kOe.

$t(\text{Cr})$ (\AA)	$M$ vs $H$ ( $\pm 0.03$ )	$J/M$ (kOe)	
		$\Delta\rho/\rho$ ( $\pm 0.03$ )	FMR ( $\pm 0.01$ )
13	0.15	0.13	0.125
13	0.14	...	0.134
14.5	0.13	0.12	0.112
16	0.32	0.26	0.292
17	0.16	0.22	0.198
18	...	0.13	0.115
20	0.16	0.20	0.150
24	0.03	0.04	0.041

Oe,  $K_u/M = 5$  Oe,  $4\pi M' = 19.0$  kG,  $J/M = 150$  Oe, and  $g = 2.09$ ) as in Fig. 1(a), we have calculated<sup>11</sup> the solid lines shown in Fig. 1(c). The very good agreement with the data obtained without any adjustment in the parameters clearly establishes  $J\hat{\mathbf{M}}_1 \cdot \hat{\mathbf{M}}_2$  as the correct antiferromagnetic coupling expression. Similar agreement is found for the  $\mathbf{H} \parallel [100]$  data. We point out that the FMR parameters used above are essentially the same as those we found for single Fe(001) films in the same thickness range.

Since we observe [Fig. 1(c)] two resonance modes for  $H > H_b$ , at much higher frequencies one also might expect to observe two FMR lines. Indeed, at 35 GHz we have found a weak satellite which is 530 Oe above the main FMR line. This is in quite good agreement with the  $4J/M$  shift one expects for  $\mathbf{H} \parallel [110]$  from Eqs. (4) and (5).

The values of  $J/M$ , determined by analyzing the three types of data discussed above, are shown for all the antiferromagnetically aligned Fe/Cr/Fe samples in Table I and the more accurate high-field FMR determined values are plotted in Fig. 2. From our examination of the data, we find no clear evidence of antiferromagnetic alignment unless the Cr thickness lies in the range  $12 < t(\text{Cr}) < 25 \text{ \AA}$ . This conclusion is in better agreement with the thickness range found earlier<sup>5</sup> for (001) superlattice samples than with that found<sup>3</sup> for (110) sandwiches.

Furthermore, Fig. 2 suggests [at least for the Fe/Cr/Fe(001) structure considered here] that the  $J/M$  dependence on  $t(\text{Cr})$  is peaked near  $t(\text{Cr}) = 16 \text{ \AA}$ . This behavior is reasonable, since as  $t(\text{Cr})$  becomes sufficiently

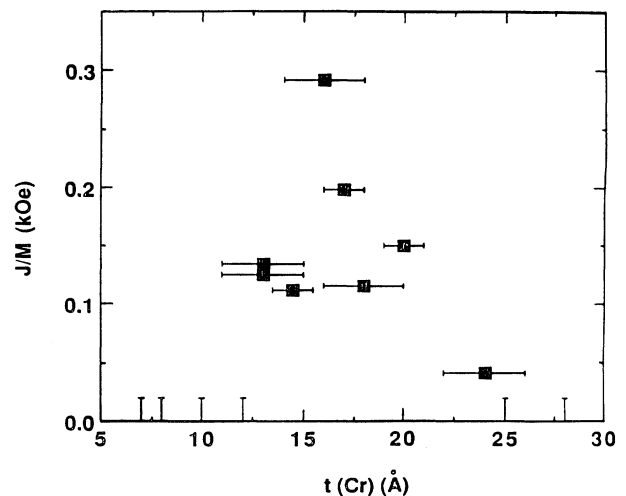


FIG. 2. Dependence of coupling parameter  $J/M$  on Cr thickness for Fe/Cr/Fe(001) samples as determined from high-field FMR. Solid squares represent samples with observed antiferromagnetic alignment. Error bars along the base line show samples which exhibited no such alignment and for which  $J/M \leq +0.02$  kOe.

large, the coupling constant  $J$  is expected to decrease based on very general arguments. On the other hand, when  $t(\text{Cr})$  vanishes, the direct exchange between the Fe layers will cause them to be ferromagnetically coupled. It is likely that interface roughness or diffusion extends this ferromagnetic coupling to finite  $t(\text{Cr})$  resulting in the apparent falloff in  $J$  at small  $t(\text{Cr})$ . This functional dependence is in clear contrast to the apparent monotonic variation in  $J$  found earlier<sup>4</sup> from the analysis of Cr/Fe(001) multilayers with  $9 < t(\text{Cr}) < 30 \text{ \AA}$ .

In summary, we have used ferromagnetic resonance to measure  $J$  directly and, in particular, have obtained from variable frequency FMR a very rich data set which any physical model must fit. Also, the  $J\hat{\mathbf{M}}_1 \cdot \hat{\mathbf{M}}_2$  form of the coupling explains all the available FMR data and, using the same parameters, predicts the location of the MR features as well as the detailed  $M$  vs  $H$  behavior. The Cr thickness dependence of  $J$  and the physical origin of  $J$  remain as outstanding theoretical problems.

We thank D. King and F. Kovanic for their excellent technical assistance and the Office of Naval Research for financial support. A.C. acknowledges support from the National Research Council.

<sup>1</sup>P. Grünberg, R. Schreiber, Y. Pang, M. B. Brodsky, and H. Sowers, Phys. Rev. Lett. **57**, 2442 (1986).

<sup>2</sup>C. Carbone and S. F. Alvarado, Phys. Rev. B **36**, 2443 (1987).

<sup>3</sup>F. Saurenbach, U. Walz, L. Hinchey, P. Grünberg, and W. Zinn, J. Appl. Phys. **63**, 3437 (1988).

<sup>4</sup>F. Nguyen Van Dau, A. Fert, P. Eitenne, M. N. Baibich, J. M. Broto, J. Chazelas, A. Friederich, S. Hadjoudj, H. Hurdequint, J. P. Radoules, and J. Massies, J. Phys. (Paris), Colloq. **49**, C8-1633 (1988).

<sup>5</sup>M. N. Baibich, J. M. Broto, A. Fert, F. Nguyen Van Dau, F. Petroff, P. Eitenne, G. Creuzet, A. Friedrich, and J. Chazelas, Phys. Rev. Lett. **61**, 2472 (1988).

<sup>6</sup>G. Binasch, P. Grünberg, F. Saurenbach, and W. Zinn, Phys. Rev. B **39**, 4828 (1989).

<sup>7</sup>J. J. Krebs, B. T. Jonker, and G. A. Prinz, J. Appl. Phys. **61**, 3744 (1987).

<sup>8</sup>T. R. McGuire and R. I. Potter, IEEE Trans. Magn. **11**, 1018 (1975).

<sup>9</sup>B. Dieny, J. Gavigan, and J. P. Rebouillat (to be published).

<sup>10</sup>J. Smit and H. G. Beljers, Philips Res. Rep. **10**, 113 (1955).

<sup>11</sup>J. J. Krebs, P. Lubitz, A. Chaiken, and G. A. Prinz (to be published).